



Published in final edited form as:

*J Invest Dermatol.* 2017 November ; 137(11): 2298–2308. doi:10.1016/j.jid.2017.07.002.

## Pro-inflammatory chemokines and cytokines dominate the blister fluid molecular signature in epidermolysis bullosa patients and affect leukocyte and stem cell migration

Vitali Alexeev<sup>1</sup>, Julio Cesar Salas-Alanis<sup>2</sup>, Francis Palisson<sup>3</sup>, Lila Mukhtarzada<sup>1</sup>, Giulio Fortuna<sup>4</sup>, Jouni Uitto<sup>1</sup>, Andy South<sup>1</sup>, and Olga Igoucheva<sup>1</sup>

<sup>1</sup>Department of Dermatology and Cutaneous Biology, Jefferson Medical College, Thomas Jefferson University, Philadelphia, PA, USA

<sup>2</sup>University of Monterrey, Monterrey, México

<sup>3</sup>Facultad de Medicina, Clínica Alemana Universidad del Desarrollo, Santiago, Chile

<sup>4</sup>Department of Diagnostic Science, Louisiana State University School of Dentistry, New Orleans, LA, USA

### Abstract

Hereditary epidermolysis bullosa (EB) is associated with skin blistering and the development of chronic non-healing wounds. Although clinical studies have shown that cell-based therapies improve wound healing, recruitment of therapeutic cells to blistering skin and to more advanced skin lesions remains a challenge. Here, we analyzed cytokines and chemokines in blister fluids (BF) of patients affected by dystrophic, junctional and simplex EB. Our analysis revealed high levels of CXCR1, CXCR2, CCR2 and CCR4 ligands, particularly dominant in dystrophic and junctional EB. *In vitro* migration assays demonstrated preferential recruitment of CCR4<sup>+</sup> lymphocytes and CXCR1<sup>+</sup>, CXCR2<sup>+</sup> and CCR2<sup>+</sup> myeloid cells toward EB-derived BF. Immunophenotyping of skin-infiltrating leukocytes confirmed substantial infiltration of the EB-affected skin with resting (CD45RA<sup>+</sup>) and activated (CD45RO<sup>+</sup>) T cells and CXCR2<sup>+</sup> CD11b<sup>+</sup> cells, many of which were identified as CD16b<sup>+</sup> neutrophils. Our studies also showed that abundance of CXCR2 ligand in BF also creates a favorable milieu for the recruitment of the CXCR2<sup>+</sup> stem cells, as validated by *in vitro* and in-matrix migration assays. Collectively, this study identified several chemotactic pathways that control the recruitment of leukocytes to the EB-associated skin lesions. These chemotactic axes could be explored for the refinement of the cutaneous homing of the therapeutic stem cells.

---

Correspondence: Olga Igoucheva, Ph.D., Department of Dermatology and Cutaneous Biology, Sydney Kimmel Medical College, Thomas Jefferson University, 233 South 10<sup>th</sup> Street, BLSB, Rm. 430, Philadelphia, PA 19107, (Tel) 215-503-5434, (Fax) 215-503-5788, Olga.Igoucheva@jefferson.edu.

**Conflict of Interest:** The authors state no conflict of interest.

**Publisher's Disclaimer:** This is a PDF file of an unedited manuscript that has been accepted for publication. As a service to our customers we are providing this early version of the manuscript. The manuscript will undergo copyediting, typesetting, and review of the resulting proof before it is published in its final citable form. Please note that during the production process errors may be discovered which could affect the content, and all legal disclaimers that apply to the journal pertain.

## Keywords

adult stem cells; blister fluids; blistering skin; chemokines; cytokines; epidermolysis bullosa; proteome; wound healing

---

## Introduction

Heritable epidermolysis bullosa (EB) is a group of mechanobullous disorders characterized by skin fragility. Based on the level of tissue separation within the dermo-epidermal basement membrane zone (BMZ), EB is divided into 4 categories: simplex (EBS), junctional (JEB), dystrophic (DEB) and Kindler syndrome (KS). Each sub-type of EB is associated with mutations in specific genes encoding proteins associated with mechanical stability of the BMZ. Despite the diversity of the phenotypic manifestations, all EB forms are accompanied by tissue separation and development of blisters and erosions following trauma to the skin. In physiological conditions, healing starts from coagulation of blood in ruptured blood vessels and release of different signaling molecules that recruit various cell types to the site of injury. This leads to an acute local inflammatory response, activation of tissue repair, regeneration, and restoration of tissue integrity.

A plethora of cytokines have been shown to participate in dynamic wound healing process, including one superfamily of small (8–15 kD) proteins called chemokines (Efron and Moldawer, 2004). Once secreted from damaged tissue, chemokines orchestrate wound healing-associated inflammation, angiogenesis and recruitment of extracellular matrix-producing cells. Wound healing studies on rodent models demonstrated that aberrant chemotactic signaling leads to the unresolved inflammation, chronic wounds, accumulation of extracellular matrix, scarring and necrosis. (Luster et al., 1998, Rennekampff et al., 2000). At present, however, only limited information is available regarding cytokines and chemokines in EB-affected skin.

In this study, we examined chemotactic signatures in blister fluid (BF) collected from patients affected by different types of EB. We identified chemotactic signals that can potentially contribute to impaired blister healing and define chemotactic axes improving recruitment of therapeutic stem cells to EB-affected skin. This work highlights the inflammatory and immune activities in the blistering skin of EB patients, thus, providing potential markers of disease activity and treatment effect.

## Results

### Plasma and blister fluids of EB-affected patients contain pro-inflammatory chemokines and cytokines

Chemokines were analyzed in plasma and BF collected from EB patients (DEB (n=59), JEB (n=6), EBS (n=10), and DDEBP (n=2) using antibody arrays. The clinical characteristics of EB patients are summarized in Table S1. Out of 38 chemokines, high levels of CXCL7, CCL5, CCL19, and CCL4 were detected in the plasma. Out of all, only CCL11, CXCL8, CCL15, CXCL7, and CXCL12 showed statistically significant difference ( $p < 0.05$ ) in plasma of EB patients when compared to healthy controls (Fig. 1a).

In the majority of BF from EB-affected patients, high levels of CCL27, CCL24, Gro-family (CXCL1, CXCL2, CXCL3), CXCL8, CXCL10, CCL2, CCL4, CCL15, CXCL7 and CCL5 were detected (Fig. 1b) independent of age, gender and blister location (data not shown). A side-by-side comparison of EB-derived fluids and control samples collected from frost-bite or burn-induced blisters of healthy donors showed a similar chemotactic pattern overall (Fig 1b). When chemotactic content of the advanced blisters (>98 h from onset) was compared to early blisters ( < 24 h from onset), the majority of early DEB and JEB blisters contained 2-3 times lower levels of chemokines than advanced blisters (Fig. 1c, Fig. S1). On the contrary, early EBS blisters contained significantly higher levels of CXCL5, Gro family chemokines, CXCL8 and CCL2 chemokines than advanced lesions. CCL15, CCL17 and CCL20 were also consistently higher in early EBS than in other EB types (Fig. 1c). To validate array data, several identified chemokines were quantified by Multi-Analyte ELISArray. Analysis confirmed high levels of CXCL8 (up to 1000 pg/ml), Gro-family chemokines (CXCL1/2/3) (up to 400 pg/ml), CCL2, CCL4 and CCL5 in EB-associated BF (Fig. 1d).

Elevated levels of cytokines such as IL-1 $\beta$ , IL-2, IL-6 and reduced levels of TNF $\alpha$  have been reported in the serum of DEB and EBS patients, suggesting that EB could be classified as a systemic inflammatory disease rather than a skin-limited disorder (Annicchiarico et al., 2015). Cytokine antibody array analysis showed that BF of all EB types share a similar profile: out of 88 examined cytokines, adiponectin (ACRP30), angiogenin and IL-6 were detected at the highest levels (Fig. 2). Levels of BDNF, EGF, ICAM-1, IGFBP-1, 2, 6, MSP $\alpha$  and osteoprotegerin were also consistently high in all EB types. BF also contained pro-inflammatory cytokines, including IL-1, IL-6, TNF $\alpha$ , IL15; however, some of these cytokines were counterbalanced by antagonistic soluble receptors, including IL-1ra and sTNF-R1 and sTNF-R2 (Fig 2).

### **Blister fluid-derived chemokines modulate leukocyte migration *in vitro***

Elevated levels of several chemokines in BF suggested that inflammatory cells expressing a restricted set of chemokine receptors could be mobilized to blistering skin and contribute to EB pathology. Thus, CXCR1 and CXCR2-expressing cells could be recruited to blistered skin by CXCL1/2/3/7/8, while CCR2<sup>+</sup> could be recruited by CCL2, CCR4<sup>+</sup> cells by CCL5, CCL17 and CCL22, and CCR3<sup>+</sup> cells by CCL5, CCL11 and CCL24 ligands (Fig 1d). To better characterize leukocyte recruitment and contribution to EB pathology and to define chemotactic axes for recruitment of therapeutic stem cells to EB-affected skin, human peripheral blood mononucleated cells (PBMC) isolated from healthy donors were used for the *in vitro* migration in Transwell chambers. A dose- and time-dependent migration of leukocytes was observed toward BF (Fig 3a, b). At 60 min, PBMC migration was substantially enhanced by adding BF into lower chambers. At 120 min, a 5-fold increase in migration was observed relative to control. Adding BF into both upper and lower chambers inhibited PBMC migration (Fig. 3b).

To define chemotactic axes directing leukocyte migration, expression of lead chemokine receptors for BF-associated chemokines was further examined by FACS. Lymphocytes that migrated to the lower chambers in response to BF during the first 60 min predominantly expressed CCR4 and CCR5 receptors for CCL2/17/22 and CCL4/5 BF-derived chemokines,

respectively (Fig. 3c, e). The majority of migrating myeloid cells expressed CXCR2, CCR2 and CXCR1, which are receptors for the most abundant BF chemokines, including CCL2, CXCL1/2/3, CXCL7 and CXCL8 (Fig. 3d, e). To identify fast-responding leukocytes, migration of lead chemokine receptor-positive cells was analyzed at 30 min. Based on side scatter/fluorescence data, the majority of migrating CXCR2<sup>+</sup> and CXCR1<sup>+</sup> cells were myeloid (Fig. 3f). This population was also highly positive for CCR2, whereas migrating lymphocytes were mostly positive for CCR4. Migrating CCR3<sup>+</sup> and CCR5<sup>+</sup> cells were also detected but to a considerably lesser extent (Fig. 3f). Taken together, these findings suggest that circulating leukocytes could be preferentially recruited to EB-affected blistering skin via engagement of CXCR1, CXCR2, CCR2 and CCR4 receptors.

### **Chemokines enhance recruitment of CXCR2<sup>+</sup> leukocytes to EB-affected skin**

Recruitment of leukocytes to the EB-affected skin was further validated on the tissue array containing samples of 3 EB types (DEB n=15; EBS n=8; JEB n=5). Indirect immunofluorescence analysis confirmed a 3- to 5-fold increase in skin-infiltrating CD45<sup>+</sup> leukocytes in all EB samples. A majority of the infiltrating cells were represented by CD45RO<sup>+</sup>, CD45RA<sup>+</sup> T cells and CD11b<sup>+</sup> myeloid cells (Fig. 4a, b). Clusters of CD45 infiltrating cells were identified as CXCR2<sup>+</sup> leukocytes, which were more predominant in blistering than non-blistering skin in all EB types (Fig. 5a, b). Moreover, in RDEB skin at least half of the CD11b<sup>+</sup> cells were identified as CXCR2<sup>+</sup> cells with at least two-thirds of them represented by CD16b<sup>+</sup>CXCR2<sup>+</sup> neutrophils (Fig. 5c, d). Overall, this analysis confirmed our *in vitro* data on leukocyte recruitment by BF-derived chemokines and suggested that only few chemokine receptors, including CXCR2, can direct leukocyte migration to EB-affected skin.

### **Blister fluid-derived chemokines induce migration of CXCR1<sup>+</sup> and CXCR2<sup>+</sup> therapeutic stem cells in collagenous matrix**

Several clinical investigations involving systemic transplantation of potentially therapeutic stem cells have reported inefficient engraftment of the cells to the cutaneous tissue (Nagy et al., 2011, Petrof et al., 2015, Wagner et al., 2010). With the aim of improving cutaneous homing of transplanted stem cells, we recently investigated chemotactic signals in a RDEB mouse model and identified several potential chemotactic axes directing stem cells to the RDEB skin (Alexeev et al., 2016). Based on this data, we hypothesize that adipose-derived stem cells (ADSC) expressing CXCR1 and/or CXCR2 receptors on the cell surface could be effectively recruited to EB-affected skin. However, our recent studies demonstrated that only a small percentage (4%-6%) of ADSC is CXCR1- and CXCR2-positive (Alexeev et al., 2016). To generate human ADSC that uniformly express candidate receptors, we stably transduced ADSC with plasmids encoding human CXCR1 and CXCR2 and showed robust expression of receptors on the surface of up to 70% of cells (Fig. S2). Then, CXCR1<sup>+</sup> and CXCR2<sup>+</sup> cells were used for *in vitro* migration assay in Transwell chambers with EB-derived BF or culture media (control). More than 30% of CXCR1<sup>+</sup> cells migrated to the lower chamber in response to BF (Fig. 6a, b). CXCR2-driven migration was more pronounced and BF concentration-dependent: more than 70% of CXCR2<sup>+</sup> ADSC migrated to the lower chamber in response to BF-derived chemokines (Fig. 6a, b).

Directional migration of the ADSC was further validated by the *in vitro* migration assay in collagenous matrix where stem cells and BF-containing collagenous layers were separated by at least 5 mm thick collagenous matrix. Forced expression of CXCR1 and CXCR2 led to a directional migration of the ADSC toward the BF-containing layer throughout the collagenous matrix against gravity (Fig. 6c). No substantial migration of the cells was detected in the absence of BF (not shown) or when unselected ADSC were used (Fig. 6c). Taken together, these studies showed that CXCR1 and CXCR2 chemokine receptors mediate directional migration of ADSC toward chemotactic gradients provided by BF-derived chemokines.

## Discussion

Chemokines play an important role in wound healing by orchestrating an intricate sequence of cellular events that are divided into inflammatory, proliferative and remodeling phases. The function of certain chemokines in wound healing (e.g. CXCL8) is well-characterized, whereas information about others is only now emerging (Hasegawa et al., 2013, Kroeze et al., 2012, Kroeze et al., 2009, van den Broek et al., 2014). There is still a substantial gap in understanding the role of chemokines in the healing of trauma-induced skin blisters and particularly in hereditary blistering disorders. Better understanding of these molecules in EB could provide opportunities for new therapeutic approaches aimed at reducing blister formation and improving cell-based therapies.

To date, several studies on EB patient-derived material have demonstrated increased levels of IL-1 $\beta$  and IL-6 in plasma and CXCL8 (IL-8) in BF of DEB and EBS patients. Increased levels of CCL2, CCL19 and CCL20 were observed in the skin of EBS mice (Annicchiarico et al., 2015, Heinemann et al., 2011, Lettner et al., 2013, Roth et al., 2009). Our prior studies also identified reduced transcription of CCL27, CSF3, CX3CL1 and CXCL14 and higher expression of CXCL18 in the non-blistering skin of JEB and DEB transgenic mice (Alexeev et al., 2013). Proteomic screens of chemotactic molecules in BF of DEB blistering mouse skin showed consistently high levels of CCL6, chemerin, CCL8, CCL9/CCL10, CCL12, CXCL1, CXCL2, CXCL12, CXCL5, and CDF (Alexeev et al., 2016). As presented here, analysis of human BF showed a somewhat similar pattern. High levels of the CXC chemokines containing Glu-Leu-Arg (ELR) motif (Gro family, CXCL5, CXCL7, and CXCL8) were detected in early blisters. In acute wound healing, these chemokines are responsible for the first step of the inflammatory phase, rapid recruitment of neutrophils (Van Damme et al., 1997), which begins within minutes to hours of wounding and typically lasts for 4 days (Romagnani et al., 2004). Contrary to the acute wound healing, advanced blisters and EB-affected skin contained high levels of the ELR chemokines (with the exception of CXCL5) and showed persistent infiltration with neutrophils. These observations suggest an abnormal initiation of blister healing.

The initial stage of the inflammatory phase of wound healing ends with the disappearance of neutrophils from the wound site through apoptosis, followed by recruitment of myeloid cells through CCL2, CCL3, CCL4, CCL5 and CCL7 chemokines during the first week after wounding (Engelhardt et al., 1998, Jackman et al., 2000, Wetzler et al., 2000). Consistent with this data, we also detected higher levels of CCL5, CCL2 and CCL4 in advanced blisters

compared to early blisters. Similar to chronic wounds (Schwarz et al., 2013), persistently high levels of these chemokines could be disadvantageous for blister healing.

Because ELR chemokines, particularly CXCL8, act as stimulators of neoangiogenesis and re-epithelialization (Engelhardt et al., 1998), it is plausible that consistently high levels of these chemokines accompanied by high level of angiogenin in BF may lead to unbalanced blister healing and development of chronic wounds in EB patients. Angiogenin possesses both ribonuclease and angiogenic activities (Gao and Xu, 2008), and it hydrolyzes RNA and modulates protein synthesis. In addition, it binds to a 42 kDa smooth muscle type alpha-actin to activate proteolytic cascades leading to degradation of the laminin and fibronectin layers of the basement membrane (Tello-Montoliu et al., 2006) and allowing endothelial cells to penetrate perivascular tissue. Although we did not find any significant differences in angiogenin level in different forms of EB by ELISA (Fig. S3), it is plausible that a consistently high level in BF is one of the precipitating factors in DEB- and JEB-associated SCC development and, along with ELR chemokines, in the development of chronic wounds.

In the remodeling phase of wound healing, chemokines could be responsible for excessive degradation of ECM through induction of matrix metalloproteinase (MMP) expression by skin resident cells and through sustained recruitment of neutrophils known to secrete various MMPs. It is particularly evident in chronic wounds exhibiting neutrophil-dependent impairment in re-epithelialization and increased ECM degradation (Dovi et al., 2003, Martin et al., 2003). Neutrophil-derived proteases like cathepsin G, elastase, and protease3 cleave elastin, fibronectin, laminin, vitronectin, and collagen IV (Witko-Sarsat et al., 2000), and they interfere with re-epithelialization and the formation of a new BMZ in the dermo-epidermal junction (Briggaman et al., 1984). Neutrophil-secreted MMPs (MMP8 (collagenase-2), MMP9 (gelatinase B) and MMP2 (gelatinase A) also interfere with BMZ formation by cleaving fibrillar collagens (MMP8) and type IV collagen (MMP2 and 9). This is underscored by high levels of active MMP8 and high gelatinase activity in chronic wounds (Bullen et al., 1995, Moor et al., 2009, Nwomeh et al., 1999, Nwomeh et al., 1998, Wysocki et al., 1993). Also, these MMPs can cleave and activate CXCL5 and CXCL8 (Tester et al., 2007) and process CCL2 to generate CCR1, 2, and 3 antagonists that inhibit leukocyte recruitment (McQuibban et al., 2002). Although our analysis demonstrated that several cytokines and chemokines could be associated with EB severity, prognostic value of these molecules requires further biostatistical evaluation and modeling in a larger cohort of patients.

Our analysis also revealed a high level of adiponectin (ACRP30) in EB-derived BF. This protein hormone modulates several metabolic processes, including glucose regulation and fatty acid oxidation (Diez and Iglesias, 2003). Since adiponectin level correlates with body fat percentage (Ukkola and Santaniemi, 2002), its presence in BF may also have a prognostic/evaluative value for EB patients, particularly children, who could be chronically malnourished with signs of subcutaneous fat depletion (Gruskay, 1988).

Presented analysis is of particular importance to the development of cell-based therapies for the treatment and management of EB. Recent clinical trials demonstrated that allotransplantation of bone marrow-derived stem cells into DEB patient alleviated some



disease-associated symptoms attributed to paracrine effects rather than donation of the therapeutic protein by donor cells to the BMZ (Nagy et al., 2011, Petrof et al., 2015, Wagner et al., 2010). In fact, inefficient recruitment of the adult stem cells to damaged skin has been documented in wound healing studies (Ojeh et al., 2015, Shingyochi et al., 2015). Previously, we analyzed BF in mouse models mimicking DEB (Fritsch et al., 2008, Heinonen et al., 1999) and identified several potential chemotactic axes for enhanced recruitment of therapeutic stem cells to blistering mouse skin (Alexeev et al., 2016). Although a side by side comparison of chemokines in mouse and human BF showed substantial differences, it is apparent that BF of both species contain high levels of CXCR1 and CXCR2 ligands and these chemokine receptors could be harnessed to drive migration of the therapeutic stem cells to blistering skin. Our current analysis of blister fluid-induced human stem cell migration *in vitro* is consistent with this notion. Proteome data are also supportive of the recent findings showing elevated CXCL12 levels in serum of EB-affected patients (Ujiiie et al., 2017). Yet, CXCL12 -CXCR4 chemotactic axis was mostly associated with dissemination of cancers to the lymph node, bone, lung, brain, and liver (Sun et al., 2010, Teicher and Fricker, 2010). In the skin, CXCL12 expression was associated with skin-infiltrating dendritic cells, pericytes, endothelial cells and fibroblasts (Avniel et al., 2006, Rezk et al., 2017), as well as with emigration of dendritic cells from the cutaneous tissue (Kabashima et al., 2007). In fact, data presented by Ujiiie et al. also demonstrate that CXCL12 expression in the EB-affected skin is mostly associated with skin infiltrating cell. Therefore, the role of CXCL12 in recruitment of cell to the skin remains to be further elucidated.

As discussed previously (Alexeev et al., 2013, 2016), migration of cells to peripheral tissues is a two-step process requiring (i) extravasation of cells from the blood stream, and (ii) migration of cells within the peripheral tissue (skin). Usually, separate sets of chemokines regulate these two processes. Extravasation of memory T cells from dermal blood vessels is mediated by CCR4 ligands (CCL17, CCL22 and CCL5) (Tubo et al., 2011), whereas migration of cells within the tissue requires activation of other receptors (e.g., CCR10) by epithelia-derived CCL27 (Alexeev et al., 2013). Separation of extravasation and in-tissue migration chemotactic signals helps restrict migration of circulating cells to the injured sites. Only few chemokines, including CXCL8, can mediate both processes by inducing rolling, diapedesis and intra-cutaneous migration (Kohda et al., 2002). Taking into account the high levels of CXCL7 (another CXCR2 ligand) in the plasma of EB-affected patients, it is also plausible that CXCL7 activates rolling of CXCR2<sup>+</sup> cells, whereas other CXCR2 ligands mediate intracutaneous migration. These findings, along with our recent animal studies (Alexeev et al., 2016), strongly support the hypothesis that a CXCR2<sup>+</sup> population of stem cells could be effectively recruited to EB-affected skin and is advantageous for cell-based EB therapy via systemic transplantation.

Collectively, robust analysis of BF- and plasma-associated chemokines and cytokines revealed a number of EB skin-associated chemotactic gradients, which may contribute to EB pathology by altering recruitment of leukocytes and creating a favorable milieu for the progression of the skin blisters to non-healing wounds. This study also revealed several chemotactic axes involving CXCR1/2 and CCR4 ligands that could be further exploited for

the effective recruitment and homing of the therapeutic stem cells to EB-affected skin and the improvement of the cells-based therapies.

## Materials and Methods

### Blister fluids and skin from EB patients

Blister fluids, blood and skin biopsies from EB patients were obtained with support from DEBRA Chile and DEBRA Mexico according to ethical committee rules and individual country's regulations. Clinical features of the patients are presented in Table S1. The study was not considered as human subject research.

### Chemokine and cytokine antibody arrays

Human Chemokine Antibody Arrays C1 and Human Cytokine Antibody Array C1000 (RayBiotech, Inc., Norcross, GA) were used to detect chemokines and cytokines in plasma and blister fluids according to manufacturer protocols. Analysis of the obtained data was done with RayBiotech Analysis Tools software.

### ELISA assay

Multi-Analyte (Qiagen, Valencia, CA) and Angiogenin (RayBiotech) ELISA assays were used to detect most common chemokines and angiogenin as devised by manufacturers.

### Cell culture

ADSC were isolated from human foreskin and characterized and cultured according to previously established protocol (Alexeev et al., 2014). PBMC were purchased from Stem Cell Technologies (Cambridge, MA) and cultured in RPMI1640 media supplemented with 10% FBS (Thermo/Fisher, Grand Island, NY).

### Fluorescence-activated cell sorting (FACS) analysis

Cells were incubated with fluorochrome-conjugated chemokine receptor-specific antibodies (BioLegend, San Diego, CA; Table S2) (Alexeev et al., 2014). Expression of chemokine receptors was assessed on Guava EasyCyte system and analyzed using GuavaSoft 2.7 software (Millipore, Billerica, MA). Gating of different leukocyte populations was done based on the assessment of side scatter (SSC) vs forward scatter (FSC).

### Histological and immunofluorescence analyses

Frozen tissues were cryosectioned and 7  $\mu$ m sections were fixed in 4% paraformaldehyde (PFA) and used for indirect immunofluorescence analysis using antigen-specific primary antibodies (Table S2). Immunocomplexes were detected with fluorochrome-labeled secondary antibodies (Thermo/Fisher, Grand Island, NY). Slides were covered with Fluorosafe reagent (Millipore, Billerica, MA) and analyzed by fluorescent microscopy.

### Nucleofection

Nucleofection of plasmids was done using Amaxa Nucleofector II system (Lonza, Basel, Switzerland) with Kit V and T-027 program.



### ***In vitro* migration in transwell chambers and collagenous matrix**

PBMC ( $3 \times 10^6$  cells) or ADSC ( $1 \times 10^6$  cells) were loaded into the top chamber of the 8- $\mu$ m pore size Transwell chambers (Corning Costar, Scranton, PA). Control or BF-containing culture media was placed into a lower chamber. Migrated cells were collected from the lower chambers and the undersides at indicated times, enumerated and used for FACS analysis. For in-matrix migration, ADSC were fluorescently labeled with Vibrant DiO dye (Thermo/Fisher) and plated in collagen gel on the bottom of the Transwell chamber. A separating collagenous layer was created on top. The migration unit was completed by creating BF-containing collagen gel on the top. Migration unit was placed into Transwell plate and incubated for 4 days under standard tissue culture condition. After fixation in formalin and freezing, 10  $\mu$ m cryosections were used for analysis.

More detailed information on material and methods is available as supplementary material.

### **Statistical analysis**

Comparison of the data was performed using Student 2-tailed *t*-test;  $p < 0.05$  was considered statistically significant.

A more detailed description of experimental procedures is given in the Supplementary Material and Methods.

### **Supplementary Material**

Refer to Web version on PubMed Central for supplementary material.

### **Acknowledgments**

We would like to thank Dystrophic Epidermolysis Bullosa Research Association (DEBRA) Mexico, DEBRA Chile and DEBRA Spain for the efforts to collect EB samples. Research reported in this publication was supported by the National Institute of Arthritis and Musculoskeletal and Skin Diseases of the National Institutes of Health under Award Number R01AR064286 (OI).

### **References**

- Alexeev V, Arita M, Donahue A, Bonaldo P, Chu ML, Igoucheva O. Human adipose-derived stem cell transplantation as a potential therapy for collagen VI-related congenital muscular dystrophy. *Stem Cell Res Ther.* 2014; 5:21. [PubMed: 24522088]
- Alexeev V, Donahue A, Uitto J, Igoucheva O. Analysis of chemotactic molecules in bone marrow-derived mesenchymal stem cells and the skin: Ccl27-Ccr10 axis as a basis for targeting to cutaneous tissues. *Cytotherapy.* 2013; 15:171–84 e1. [PubMed: 23321329]
- Alexeev V, Donahue A, Uitto J, Igoucheva O. Chemotaxis-driven disease-site targeting of therapeutic adult stem cells in dystrophic epidermolysis bullosa. *Stem Cell Res Ther.* 2016; 7:124. [PubMed: 27568180]
- Annicchiarico G, Morgese MG, Esposito S, Lopalco G, Lattarulo M, Tampoia M, et al. Proinflammatory Cytokines and Antiskin Autoantibodies in Patients With Inherited Epidermolysis Bullosa. *Medicine (Baltimore).* 2015; 94:e1528. [PubMed: 26496255]
- Avniel S, Arik Z, Maly A, Sagie A, Basst HB, Yahana MD, et al. Involvement of the CXCL12/CXCR4 pathway in the recovery of skin following burns. *J Invest Dermatol.* 2006; 126:468–76. [PubMed: 16385346]

- Briggaman RA, Schechter NM, Fraki J, Lazarus GS. Degradation of the epidermal-dermal junction by proteolytic enzymes from human skin and human polymorphonuclear leukocytes. *J Exp Med*. 1984; 160:1027–42. [PubMed: 6384417]
- Bullen EC, Longaker MT, Updike DL, Benton R, Ladin D, Hou Z, et al. Tissue inhibitor of metalloproteinases-1 is decreased and activated gelatinases are increased in chronic wounds. *J Invest Dermatol*. 1995; 104:236–40. [PubMed: 7829879]
- Diez JJ, Iglesias P. The role of the novel adipocyte-derived hormone adiponectin in human disease. *Eur J Endocrinol*. 2003; 148:293–300. [PubMed: 12611609]
- Dovi JV, He LK, DiPietro LA. Accelerated wound closure in neutrophil-depleted mice. *J Leukoc Biol*. 2003; 73:448–55. [PubMed: 12660219]
- Efron PA, Moldawer LL. Cytokines and wound healing: the role of cytokine and anticytokine therapy in the repair response. *J Burn Care Rehabil*. 2004; 25:149–60. [PubMed: 15091141]
- Engelhardt E, Toksoy A, Goebeler M, Debus S, Bocker EB, Gillitzer R. Chemokines IL-8, GROalpha, MCP-1, IP-10, and Mig are sequentially and differentially expressed during phase-specific infiltration of leukocyte subsets in human wound healing. *Am J Pathol*. 1998; 153:1849–60. [PubMed: 9846975]
- Fritsch A, Loeckermann S, Kern JS, Braun A, Bosl MR, Bley TA, et al. A hypomorphic mouse model of dystrophic epidermolysis bullosa reveals mechanisms of disease and response to fibroblast therapy. *J Clin Invest*. 2008; 118:1669–79. [PubMed: 18382769]
- Gao X, Xu Z. Mechanisms of action of angiogenin. *Acta Biochim Biophys Sin (Shanghai)*. 2008; 40:619–24. [PubMed: 18604453]
- Gruskay DM. Nutritional management in the child with epidermolysis bullosa. *Arch Dermatol*. 1988; 124:760–1. [PubMed: 3284474]
- Hasegawa M, Higashi K, Matsushita T, Hamaguchi Y, Saito K, Fujimoto M, et al. Dermokine inhibits ELR(+)/CXC chemokine expression and delays early skin wound healing. *J Dermatol Sci*. 2013; 70:34–41. [PubMed: 23428944]
- Heinemann A, He Y, Zimina E, Boerries M, Busch H, Chmel N, et al. Induction of phenotype modifying cytokines by FERMT1 mutations. *Hum Mutat*. 2011; 32:397–406. [PubMed: 21309038]
- Heinonen S, Mannikko M, Klement JF, Whitaker-Menezes D, Murphy GF, Uitto J. Targeted inactivation of the type VII collagen gene (Col7a1) in mice results in severe blistering phenotype: a model for recessive dystrophic epidermolysis bullosa. *J Cell Sci*. 1999; 112(Pt 21):3641–8. [PubMed: 10523500]
- Jackman SH, Yoak MB, Keerthy S, Beaver BL. Differential expression of chemokines in a mouse model of wound healing. *Ann Clin Lab Sci*. 2000; 30:201–7. [PubMed: 10807166]
- Kabashima K, Shiraishi N, Sugita K, Mori T, Onoue A, Kobayashi M, et al. CXCL12-CXCR4 engagement is required for migration of cutaneous dendritic cells. *Am J Pathol*. 2007; 171:1249–57. [PubMed: 17823289]
- Kohda F, Koga T, Uchi H, Urabe K, Furue M. Histamine-induced IL-6 and IL-8 production are differentially modulated by IFN-gamma and IL-4 in human keratinocytes. *J Dermatol Sci*. 2002; 28:34–41. [PubMed: 11916128]
- Kroeze KL, Boink MA, Sampat-Sardjoepersad SC, Waaijman T, Scheper RJ, Gibbs S. Autocrine regulation of re-epithelialization after wounding by chemokine receptors CCR1, CCR10, CXCR1, CXCR2, and CXCR3. *J Invest Dermatol*. 2012; 132:216–25. [PubMed: 21850025]
- Kroeze KL, Jurgens WJ, Doulabi BZ, van Milligen FJ, Scheper RJ, Gibbs S. Chemokine-mediated migration of skin-derived stem cells: predominant role for CCL5/RANTES. *J Invest Dermatol*. 2009; 129:1569–81. [PubMed: 19122644]
- Lettner T, Lang R, Klausegger A, Hainzl S, Bauer JW, Wally V. MMP-9 and CXCL8/IL-8 are potential therapeutic targets in epidermolysis bullosa simplex. *PLoS One*. 2013; 8:e70123. [PubMed: 23894602]
- Luster AD, Cardiff RD, MacLean JA, Crowe K, Granstein RD. Delayed wound healing and disorganized neovascularization in transgenic mice expressing the IP-10 chemokine. *Proc Assoc Am Physicians*. 1998; 110:183–96. [PubMed: 9625525]

- Martin P, D'Souza D, Martin J, Grose R, Cooper L, Maki R, et al. Wound healing in the PU.1 null mouse--tissue repair is not dependent on inflammatory cells. *Curr Biol*. 2003; 13:1122–8. [PubMed: 12842011]
- McQuibban GA, Gong JH, Wong JP, Wallace JL, Clark-Lewis I, Overall CM. Matrix metalloproteinase processing of monocyte chemoattractant proteins generates CC chemokine receptor antagonists with anti-inflammatory properties in vivo. *Blood*. 2002; 100:1160–7. [PubMed: 12149192]
- Moor AN, Vachon DJ, Gould LJ. Proteolytic activity in wound fluids and tissues derived from chronic venous leg ulcers. *Wound Repair Regen*. 2009; 17:832–9. [PubMed: 19903304]
- Nagy N, Almaani N, Tanaka A, Lai-Cheong JE, Techanukul T, Mellerio JE, et al. HB-EGF induces COL7A1 expression in keratinocytes and fibroblasts: possible mechanism underlying allogeneic fibroblast therapy in recessive dystrophic epidermolysis Bullosa. *J Invest Dermatol*. 2011; 131:1771–4. [PubMed: 21471992]
- Nwomeh BC, Liang HX, Cohen IK, Yager DR. MMP-8 is the predominant collagenase in healing wounds and nonhealing ulcers. *J Surg Res*. 1999; 81:189–95. [PubMed: 9927539]
- Nwomeh BC, Yager DR, Cohen IK. Physiology of the chronic wound. *Clin Plast Surg*. 1998; 25:341–56. [PubMed: 9696897]
- Ojeh N, Pastar I, Tomic-Canic M, Stojadinovic O. Stem Cells in Skin Regeneration, Wound Healing, and Their Clinical Applications. *Int J Mol Sci*. 2015; 16:25476–501. [PubMed: 26512657]
- Petrof G, Lwin SM, Martinez-Queipo M, Abdul-Wahab A, Tso S, Mellerio JE, et al. Potential of Systemic Allogeneic Mesenchymal Stromal Cell Therapy for Children with Recessive Dystrophic Epidermolysis Bullosa. *J Invest Dermatol*. 2015; 135:2319–21. [PubMed: 25905587]
- Rennekampff HO, Hansbrough JF, Kiessig V, Dore C, Sticherling M, Schroder JM. Bioactive interleukin-8 is expressed in wounds and enhances wound healing. *J Surg Res*. 2000; 93:41–54. [PubMed: 10945942]
- Rezk AF, Kemp DM, El-Domyati M, El-Din WH, Lee JB, Uitto J, et al. Misbalanced CXCL12 and CCL5 chemotactic signals in vitiligo onset and progression. *J Invest Dermatol*. 2017
- Romagnani P, Lasagni L, Annunziato F, Serio M, Romagnani S. CXC chemokines: the regulatory link between inflammation and angiogenesis. *Trends Immunol*. 2004; 25:201–9. [PubMed: 15039047]
- Roth W, Reuter U, Wohlenberg C, Bruckner-Tuderman L, Magin TM. Cytokines as genetic modifiers in K5-/- mice and in human epidermolysis bullosa simplex. *Hum Mutat*. 2009; 30:832–41. [PubMed: 19267394]
- Schwarz F, Jennewein M, Bubel M, Holstein JH, Pohlemann T, Oberringer M. Soft tissue fibroblasts from well healing and chronic human wounds show different rates of myofibroblasts in vitro. *Mol Biol Rep*. 2013; 40:1721–33. [PubMed: 23065295]
- Shingyochi Y, Orbay H, Mizuno H. Adipose-derived stem cells for wound repair and regeneration. *Expert Opin Biol Ther*. 2015; 15:1285–92. [PubMed: 26037027]
- Sun X, Cheng G, Hao M, Zheng J, Zhou X, Zhang J, et al. CXCL12 / CXCR4 / CXCR7 chemokine axis and cancer progression. *Cancer Metastasis Rev*. 2010; 29:709–22. [PubMed: 20839032]
- Teicher BA, Fricker SP. CXCL12 (SDF-1)/CXCR4 pathway in cancer. *Clin Cancer Res*. 2010; 16:2927–31. [PubMed: 20484021]
- Tello-Montoliu A, Patel JV, Lip GY. Angiogenin: a review of the pathophysiology and potential clinical applications. *J Thromb Haemost*. 2006; 4:1864–74. [PubMed: 16961595]
- Tester AM, Cox JH, Connor AR, Starr AE, Dean RA, Puente XS, et al. LPS responsiveness and neutrophil chemotaxis in vivo require PMN MMP-8 activity. *PLoS One*. 2007; 2:e312. [PubMed: 17375198]
- Tube NJ, McLachlan JB, Campbell JJ. Chemokine receptor requirements for epidermal T-cell trafficking. *Am J Pathol*. 2011; 178:2496–503. [PubMed: 21641376]
- Ujii I, Fujita Y, Nakayama C, Matsumura W, Suzuki S, Shinkuma S, et al. Altered balance of epidermis-related chemokines in epidermolysis bullosa. *J Dermatol Sci*. 2017
- Ukkola O, Santaniemi M. Adiponectin: a link between excess adiposity and associated comorbidities? *J Mol Med (Berl)*. 2002; 80:696–702. [PubMed: 12436346]

- Van Damme J, Wuyts A, Froyen G, Van Coillie E, Struyf S, Billiau A, et al. Granulocyte chemotactic protein-2 and related CXC chemokines: from gene regulation to receptor usage. *J Leukoc Biol.* 1997; 62:563–9. [PubMed: 9365109]
- van den Broek LJ, Kroeze KL, Waaijman T, Breetveld M, Sampat-Sardjoeipersad SC, Niessen FB, et al. Differential response of human adipose tissue-derived mesenchymal stem cells, dermal fibroblasts, and keratinocytes to burn wound exudates: potential role of skin-specific chemokine CCL27. *Tissue Eng Part A.* 2014; 20:197–209. [PubMed: 23980822]
- Wagner JE, Ishida-Yamamoto A, McGrath JA, Hordinsky M, Keene DR, Woodley DT, et al. Bone marrow transplantation for recessive dystrophic epidermolysis bullosa. *N Engl J Med.* 2010; 363:629–39. [PubMed: 20818854]
- Wetzler C, Kampfer H, Pfeilschifter J, Frank S. Keratinocyte-derived chemotactic cytokines: expressional modulation by nitric oxide in vitro and during cutaneous wound repair in vivo. *Biochem Biophys Res Commun.* 2000; 274:689–96. [PubMed: 10924337]
- Witko-Sarsat V, Rieu P, Descamps-Latscha B, Lesavre P, Halbwachs-Mecarelli L. Neutrophils: molecules, functions and pathophysiological aspects. *Lab Invest.* 2000; 80:617–53. [PubMed: 10830774]
- Wysocki AB, Staiano-Coico L, Grinnell F. Wound fluid from chronic leg ulcers contains elevated levels of metalloproteinases MMP-2 and MMP-9. *J Invest Dermatol.* 1993; 101:64–8. [PubMed: 8392530]

## Abbreviations

<b>ADSC</b>	adipose-derived stem cells
<b>BF</b>	blister fluids
<b>BMZ</b>	basement membrane zone
<b>DEB</b>	dystrophic epidermolysis bullosa
<b>EB</b>	epidermolysis bullosa
<b>EBS</b>	epidermolysis bullosa simplex
<b>JEB</b>	junctional epidermolysis bullosa
<b>DDEB-pr</b>	Dominant Dystrophic Epidermolysis Bullosa Pruriginosa
<b>PBMC</b>	peripheral blood mononucleated cells

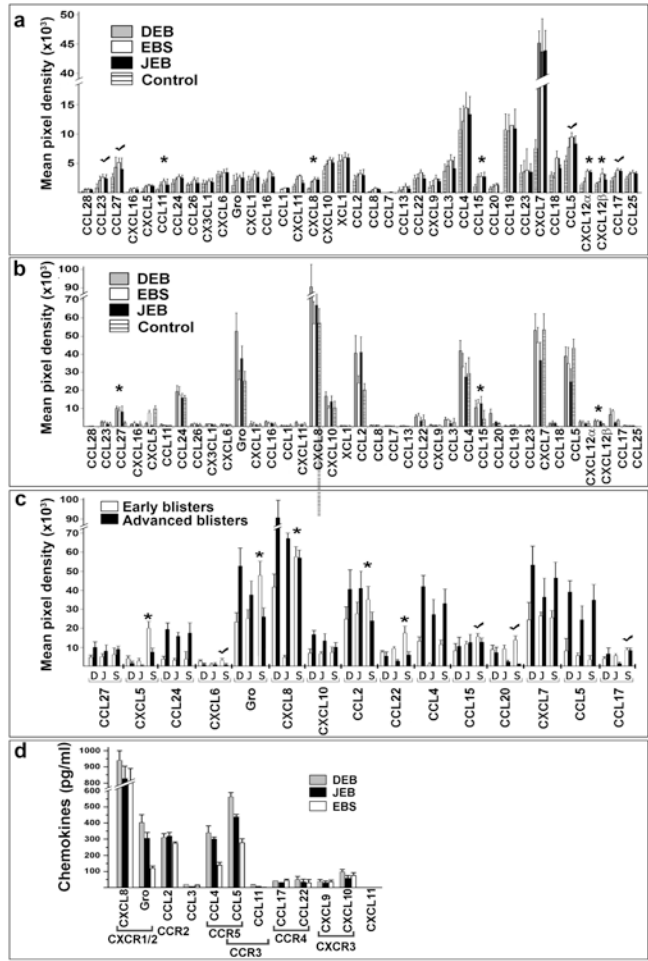


**Figure 1. Proteomic screens of chemokines in plasma and blister fluids of EB-affected patients** (a-c) Antibody array analysis of the chemokines in plasma (a) and blister fluids (b, c) of EB affected patients. Asterisks indicate chemokines which levels are significantly different ( $p < 0.05$ ) in EB samples relative to control. Check marks indicate consistently high chemokines. Panel a - blood plasma from healthy donors was used as a control. Panel (b) - blister fluids from frost bite-and burn-induced blisters of healthy donors was used as a control. The data was collected from independent arrays with duplicate measurements for each chemokine using all samples listed in Table S1. Data are presented as a mean pixel density  $\pm$  SD. EB types are indicated in the inserts. (c) Comparison of the selected chemotactic molecules in early and advanced blisters of EB patients. EB forms (DEB (D), JEB (J) and EBS (S)) and chemokines are listed below the columns. (d) Multi-Analyte ELISA analysis of common human chemokines in selected DEB (n=18), JEB (n=6) and EBS (n=6) BF samples. The values are presented as the mean chemokine concentration (pg/ml)  $\pm$  SD. Detected chemokines and their cognate receptors are shown below the columns.

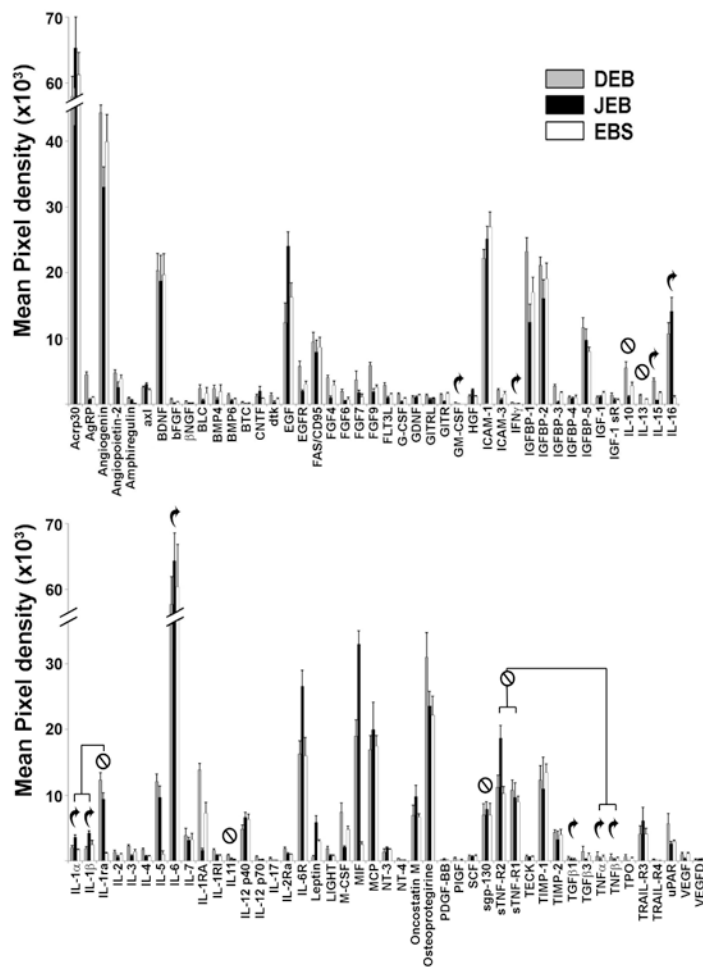


**Figure 2. Proteome analysis of cytokines in blister fluids of EB-affected patients**  
 The 88 most common cytokines were assessed in BF by protein array analysis. Cytokines are listed below the columns. Data are presented as a mean pixel density  $\pm$  SD. EB types are indicated in the insert. Curved arrows are placed above typical pro-inflammatory cytokines and crossed circles are placed above typical anti-inflammatory cytokines.



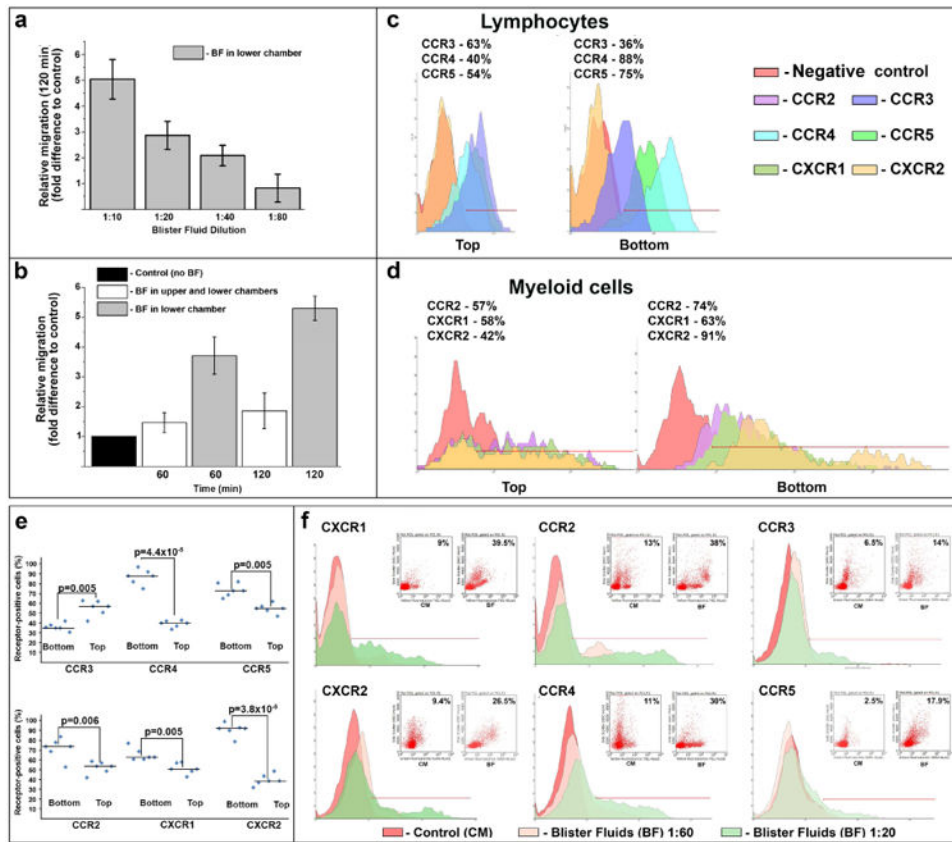


**Figure 3. EB blister fluid-derived chemokines affect leukocyte migration *in vitro***  
 (a, b) Concentration (a) and time-dependent (b) BF-induced leukocyte migration in Transwell migration chambers. Dilution of BF and time indicated below the columns. Conditions are shown on panel inserts. The data were collected from three independent experiments in triplicate and presented as migration (fold difference) relative to control (culture media in both chambers)  $\pm$  SD. (c, d) FACS-based analysis of selected chemokine receptors on BF-responding lymphocytes (c) and myeloid cells (d). Representative profiles illustrate chemokine receptor-positive cells retained in the top chamber (Top) or migrated to the lower chamber and the underside (Bottom) of Transwell migration chamber within 60 min. Detected chemokine receptors are shown on the inserts. Percentage of receptor-positive cells is shown above the profiles. (e) Scatter plots showing percentage and median of chemokine receptor-positive translocated (Bottom) and sessile (Top) cells depicted on panels c and d. Statistical significance (p-value) is shown above the plots. (f) Short-term analysis of selected chemokine receptor-positive populations migrated in Transwell chambers in response to BF at 1:20 and 1:60 dilutions (as indicated) within 30 min. Detected chemokine receptors are shown above representative histograms. Inserts show distribution of receptor-positive populations (side scatter/fluorescence) exposed to culture media (CM) and blister fluid (BF). Percentage of migrated chemokine-receptor-positive population is shown in inserts. Histogram markers define a threshold of chemokine-receptor positive cells.

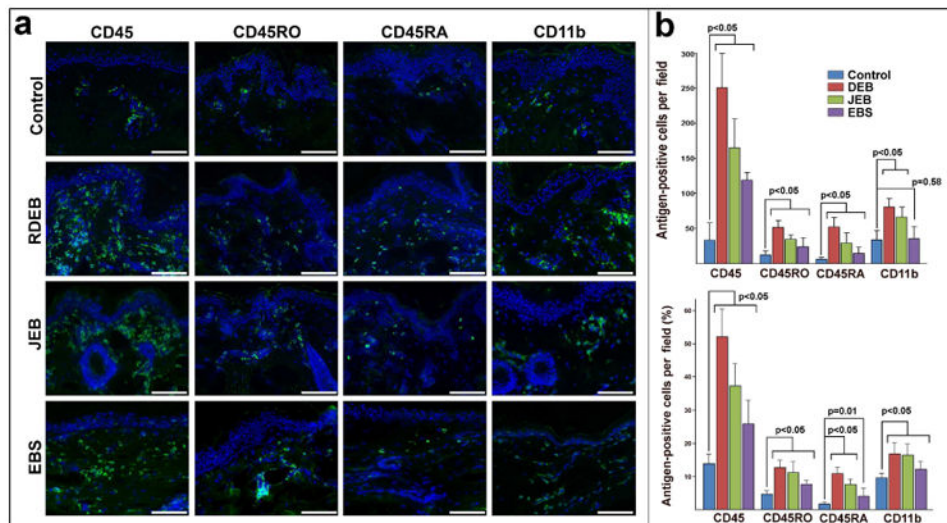


**Figure 4. EB-affected skin is infiltrated with T lymphocytes and myeloid cells**

(a) Immuno-phenotyping of infiltrating leukocytes in normal (control) and non-blistering EB-affected skin using CD45, CD45RO, CD45RA and CD11b antibodies (green). EB types appear to the left of the micrographs. Detected antigens appear on the top. Blue - DAPI nuclei staining. Scale bar - 100  $\mu$ m. (b) Quantitation of skin-infiltrating CD45RO<sup>+</sup> and CD45RA<sup>+</sup> T cells and CD11b<sup>+</sup> myeloid cells. Analysis was done on 5 random sections from 3 independent biopsies of control and EB-affected skin. Data are presented as number and percentage of antigen-positive cells per microscopic field  $\pm$  SD. Infiltration was compared using *t*-test. *p*-value < 0.05 was considered statistically significant.

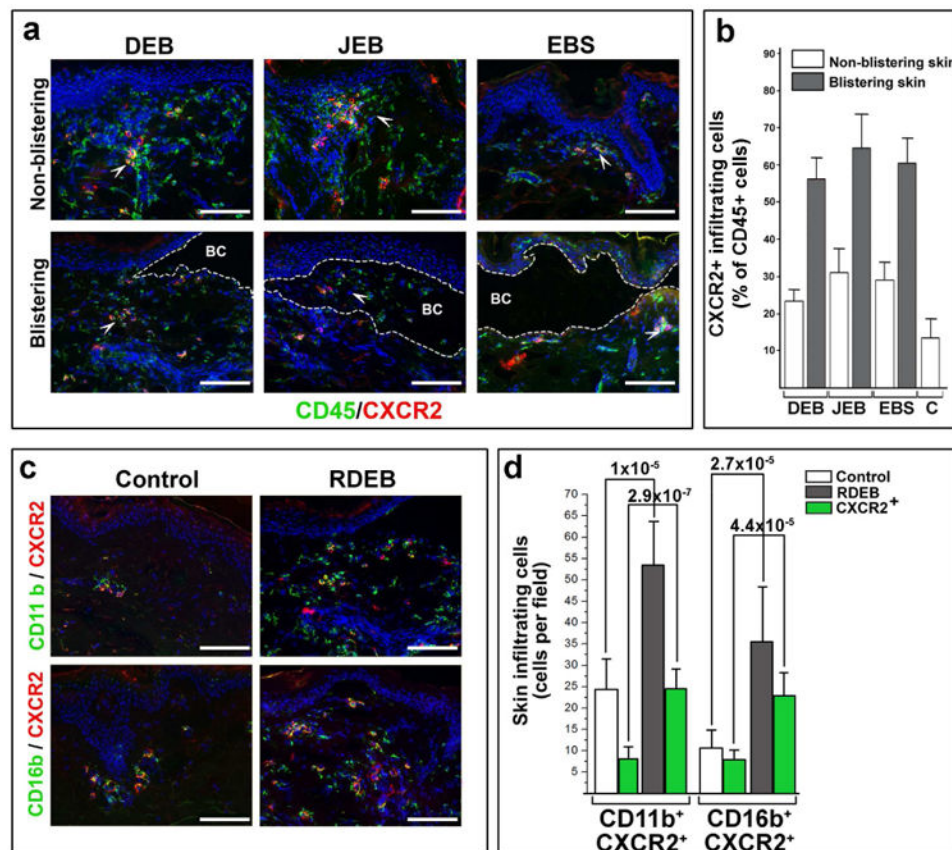


### Figure 5. EB-affected skin is infiltrated with CXCR2<sup>+</sup> leukocytes

Infiltration of the DEB, JEB and EBS-affected blistering and non-blistering skin with CD45<sup>+</sup> and CXCR2<sup>+</sup> leukocytes. EB types are indicated above representative images. Detected antigens (in corresponding color) are shown at the bottom of the panel. The blister cavity (BC) is outlined by dotted line. White arrowheads point to representative groups of CD45<sup>+</sup> CXCR2<sup>+</sup> leukocytes. Quantitation of lymphocytic infiltrate in control (C) and EB-affected skin was done on 10 random microscopic fields of blistering and non-blistering skin for each EB type, averaged and presented as a percentage of CD45<sup>+</sup> cells per microscopic field  $\pm$  SD. Skin phenotype is shown in inserts. All samples achieved statistical significance when compared to control skin ( $p < 0.05$ ). (c) Characterization of skin-infiltrating CXCR2<sup>+</sup> cells in control and RDEB-affected skin. Detected antigens (in respective colors) are shown to the left of the panels. On all representative images: Blue - DAPI nuclear staining; Scale bar - 100  $\mu$ m. Single channel images are presented in Supplementary materials (Figs. S5a and S5c). (d) Quantitation of CXCR2<sup>+</sup>-infiltrating leukocytes in control and RDEB-affected skin (shown in inserts). The data are presented as a mean number of antigen-positive cells (shown below the columns) per microscopic field  $\pm$  SD. Statistical significance (p-value) is shown above the columns.

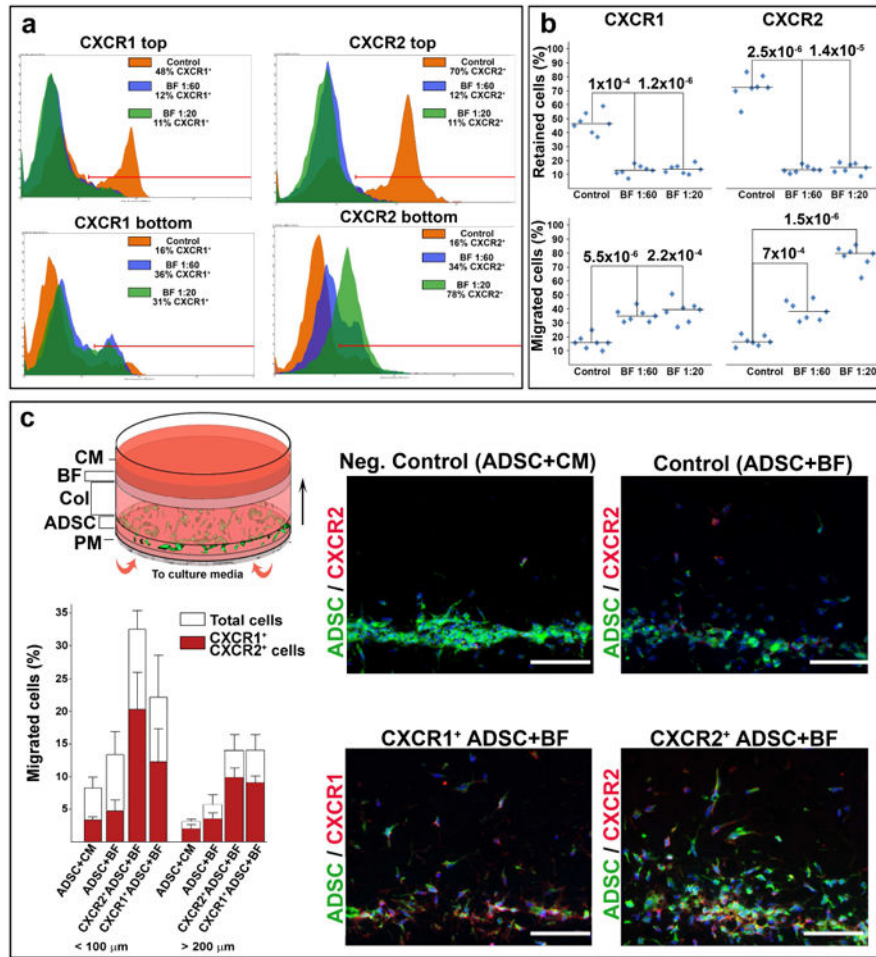


**Figure 6. EB-derived blister fluids support migration of CXCR1<sup>+</sup> and CXCR2<sup>+</sup> ADSC**  
 (a) Representative FACS profiles of CXCR1<sup>+</sup> and CXCR2<sup>+</sup> ADSC in the Transwell migration assay. Percentage of retaining (top chamber) and migrated (bottom chamber) cells is indicated in inserts: Orange - cell migration without BF (Control); Blue and Green - cell migration toward BF at 1:20 and 1:60 dilution, respectively. Histogram markers define a threshold of chemokine-receptor positive cells. (b) Analysis of retaining and migrating CXCR1<sup>+</sup> and CXCR2<sup>+</sup> ADSC in the Transwell chambers. Data were collected from 2 independent experiments in triplicates. Data are presented as scatter plots depicting percentage of CXCR1<sup>+</sup> and CXCR2<sup>+</sup> cells. Statistical significance (p-value) is shown above the plots. (c) Analysis of BF-induced ADSC migration in collagenous matrix. Top left - scheme of the in-matrix migration unit. PM - porous membrane; ADSC - ADSC-containing collagenous gel; Col - separating collagenous layer; BF - blister fluid-containing collagenous gel; CM - culture media. Arrow indicates direction of migration. Representative images of cross sections of migration units are shown on the right: top row - migration of the unselected ADSC toward culture media (CM) and blister fluids (BF); bottom row - migration of CXCR1<sup>+</sup> and CXCR2<sup>+</sup> ADSC toward BF. Blue - DAPI nuclear staining; Green - vibrant DiO-labeled ADSC; Red - CXCR1<sup>+</sup> or CXCR2<sup>+</sup> ADSC detected by indirect immunofluorescence. Scale bar - 100 μm. Single channel images are presented in Supplementary materials (Fig. S6c). Bottom left - quantitative assessment of ADSC

migration in collagenous matrix. Migration is calculated as percentage of total (open columns) and CXCR1- or CXCR2-positive (red columns) ADSC migrated less than 100 or more than 200  $\mu\text{m}$  per microscopic field  $\pm$  SD. Conditions are indicated below the columns.

Author Manuscript

Author Manuscript

Author Manuscript

Author Manuscript